

# ObjectRelator: Enabling Cross-View Object Relation Understanding in Ego-Centric and Exo-Centric Videos

Yuqian Fu<sup>1</sup>, Runze Wang<sup>2</sup>, Yanwei Fu<sup>2</sup>, Danda Pani Paudel<sup>1</sup>, Xuanjing Huang<sup>2</sup>, Luc Van Gool<sup>1</sup>  
<sup>1</sup>INSAIT, Sofia University, “St. Kliment Ohridski”, Bulgaria <sup>2</sup>Fudan University, China

## Abstract

In this paper, we focus on the Ego-Exo Object Correspondence task, an emerging challenge in the field of computer vision that aims to map objects across ego-centric and exo-centric views. We introduce ObjectRelator, a novel method designed to tackle this task, featuring two new modules: Multimodal Condition Fusion (MCFuse) and SSL-based Cross-View Object Alignment (XObjAlign). MCFuse effectively fuses language and visual conditions to enhance target object localization, while XObjAlign enforces consistency in object representations across views through a self-supervised alignment strategy. Extensive experiments demonstrate the effectiveness of ObjectRelator, achieving state-of-the-art performance on Ego2Exo and Exo2Ego tasks with minimal additional parameters. This work provides a foundation for future research in comprehensive cross-view object relation understanding highlighting the potential of leveraging multimodal guidance and cross-view alignment. Codes and models will be released to advance further research in this direction.

## 1. Introduction

Advancements in video applications, including classification [21, 41, 62], captioning [15, 25, 64], and generation [54, 57, 61], have largely focused on **exo-centric (third-person)** videos. In contrast, progress on **ego-centric (first-person)** videos, crucial for fields like virtual reality and robotics, are relatively behind. Essentially, most efforts have concentrated on developing ego-centric models [4, 9, 24, 33, 58, 65] to bridge ego- and exo-centric video understanding, while fewer studies [39, 48, 55] have explored the relationships between the two views directly, due to the lack of cross-view datasets. The recent release of the **Ego-Exo4D** dataset [10], a large-scale, temporally aligned ego-exo dataset, enables the study of **cross-view object relation understanding**, offering a promising approach to bridging the ego-exo gap.

Specifically, in this paper, we tackle the task of **Ego-**

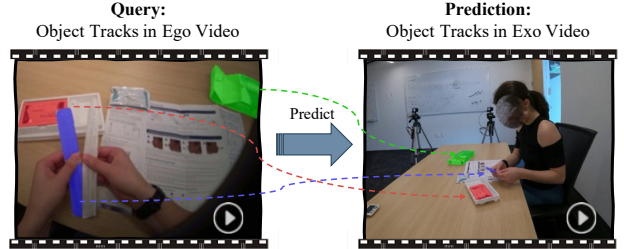


Figure 1. Illustration of the Ego-Exo Object Correspondence Task (example shown: Ego2Exo).

**Exo Object Correspondence**<sup>1</sup>, first introduced in Ego-Exo4D [10]. As shown in Fig.1, given object queries from one perspective (e.g., ego view), the task involves predicting the corresponding object masks in another perspective (e.g., exo view). Unlike prior segmentation tasks [12, 22, 27, 46, 69], which use categories, text descriptions, or visual hints as prompts, this task focuses on cross-view object understanding, utilizing visual cues from one perspective to predict the corresponding objects in a completely different perspective. This makes the direct application of existing methods nontrivial. Critically, few studies have explored ego-exo object correspondence, with PSALM [68] standing out as a notable exception. Particularly, PSALM [68] integrates Mask2Former [1] with large language models (LLMs), outperforming flagship segmentation models e.g., LISA [27], SEEM [69], and SAM [23], while also enabling zero-shot learning (ZSL) on the ego-exo object correspondence task.

However, despite its state-of-the-art performance on other segmentation tasks, PSALM faces challenges with the ego-exo object correspondence task due to two key limitations: 1) Relying solely on object masks underutilizes semantic information, limiting the LLM’s language understanding. For instance, it may segment objects with similar shapes to the query but incorrect categories. 2) PSALM does not account for the cross-view relationships between objects in ego-exo scenarios, causing it to fail when sig-

<sup>1</sup>Originally termed “Ego-Exo Correspondence” in Ego-Exo4D [10]. Renamed for clarity, emphasizing object-level mapping.

nificant visual appearance shifts are observed. These challenges raise two critical questions: ① Can incorporating language conditions with mask queries improve object localization? ② Can we ensure consistency across perspectives for the same objects?

To address these key challenges, we propose two innovative modules. First, the Multimodal Condition Fusion (MCFuse) module is proposed to tackle the question ①. While the task provides only object query masks, MCFuse enhances this by incorporating semantic information from large vision-language models like LLaVA [35], which generates language descriptions of the query object. We then combine both the object mask and the generated text in the embedding space using a lightweight cross-attention mechanism with residual connection and learnable fusion weight. This fusion enables the model to leverage both visual and linguistic cues, leading to more accurate localization of the target object. Next, to deal with question ②, we introduce the Cross-View Object Alignment (XObjAlign) module. This module aligns paired ego and exo object masks into a shared latent space, enforcing proximity between them. Utilizing an effective self-supervised learning approach, we optimize the distance similarity between the masks, which helps the model better recognize objects across different perspectives and overcome challenges posed by view changes.

By integrating MCFuse and XObjAlign into the PSALM framework, we present our method, **ObjectRelator**. We demonstrate the effectiveness of our approach through extensive experiments on both Ego2Exo and Exo2Ego tasks, achieving state-of-the-art (SOTA) performance with 0.26M additional learnable parameters surpassing the base PSALM by over 10%. Moreover, we showcase the flexibility of ObjectRelator by investigating both joint training and single-condition testing capabilities, highlighting its adaptability to various settings and scenarios.

We summarize our contributions as, 1) *Ego-Exo Object Correspondence Task*: Early exploration of the challenging task is performed highlighting its unique difficulties from traditional segmentation. 2) *Multimodal Condition Fusion (MCFuse)*: MCFuse enhances object localization by effectively combining visual and linguistic cues, using language descriptions from vision-language models. 3) *Cross-View Object Alignment (XObjAlign)*: XObjAlign ensures consistency across ego and exo perspectives, improving the model’s robustness to view changes. 4) *ObjectRelator Framework*: By integrating MCFuse and XObjAlign, we develop the novel ObjectRelator, achieving state-of-the-art results on both Ego2Exo and Exo2Ego tasks. 5) *Flexibility and Adaptability*: We demonstrate ObjectRelator’s flexibility via joint training and single-condition testing.

## 2. Related Work

**Ego-Exo Video Understanding.** Both ego- and exo-centric video perspectives are crucial for understanding the world. Extensive work has been done in single-view video understanding: For ego-centric videos, numerous methods address tasks such as video classification [8, 21, 41, 62], captioning [15, 25, 64], video generation [54, 57, 61]. While ego-centric research has historically lagged behind exo-centric, recent efforts including datasets such as Ego4D [9], EK100 [4], HoloAssist [58], AssistQ [60], as well as a variety of methods [7, 19, 24, 32, 33, 43, 65, 66] have brought substantial progress. However, far fewer studies directly address the relationship between ego and exo views. Notable exceptions have ego-exo translation/generation [2, 36, 38, 39, 55]. One factor leading to this gap is that existing datasets are often small in scale or lack comprehensive annotations [5, 14, 18, 26, 44, 50, 53]. Recently, the release of Ego-Exo4D [10], a large-scale, richly annotated, and time-synchronized multimodal dataset, has opened new chances for advancing ego-exo research. In this paper, we focus on the ego-exo object correspondence task proposed in Ego-Exo4D, aiming to establish a strong starting point with our approach.

**Segmentation Models.** Segmentation models can roughly be grouped into several main categories based on their input types: generic segmentation, referring segmentation, and interactive segmentation. We refer to generic segmentation [40] as those more classical segmentation tasks e.g., semantic segmentation [28], instance segmentation [11], and panoptic segmentation [22]. Generic segmentation methods don’t need extra text prompts or visual prompts, for example, Mask-RCNN [12] and Mask2Former [1]. In contrast, referring segmentation [17] requires textual descriptions to guide the segmentation. Flagship examples include LISA [27], GLAMM [46], PixelLM [49]. The interactive segmentation [45] utilizes visual hints or prompts such as bounding boxes, key points, or masks provided within the image to guide the segmentation results. Well-known examples have OMG-Seg [30], SAM [23], SAM2 [47]. The latest advancements such as UNINEXT [63], SEEM [69], PSALM [68] accept multiple conditions as input, which we termed as “Universal Segmentation”. However, none of them are specifically tailored for the ego-exo object correspondence, which is essentially challenged by the huge view change between the first-person and third-person observations. Thus, how to build a good segmentation model for this new task still remains uncovered.

Differences of methods are summarized in Tab.1. Typically, SAM [23], OMG-Seg [30], and SAM2 [47] decode visual prompts solely from hints such as points, masks, and bounding boxes, without referencing the corresponding image. These approaches require strict alignment between the mask and testing image, limiting adaptability for

Methods	Task	Extra Prompts	Cross-View	Comparable to Ours
Mask-RCNN [12], Mask2Former [1]	Generic Segmentation	$\times$	$\times$	$\times$
LISA [27], GLAMM [46], PixelLM [49]	Referring Segmentation	Text Descriptions	$\times$	$\times$
SAM [23], OMG-Seg [30], SAM2 [47]	Interactive Segmentation	Visual Prompts, Prompt Decoder w/o referring to image	$\times$	$\times$
UNINEXT [63], SEEM [69], PSALM [68]	Universal Segmentation	Text/Visual Prompts, Prompt Decoder with referring to image	$\times$	$\checkmark$
<b>ObjectRelator (Ours)</b>	<b>Ego-Exo Object Correspondence</b>	Text+Visual Prompts, Prompt Decoder with referring to image	$\checkmark$	-

Table 1. Comparison of tasks and methods. Note that prompt decoder choice depends on the method, not necessarily linked to the task.

tasks like ours, where object locations and shapes vary inherently. By contrast, UNINEXT [63], SEEM [69], and PSALM [68] decode visual prompts with image reference, making them more comparable to our method. Importantly, we differ from existing segmentation approaches by focusing on cross-view challenges and exploring the fusion of multiple conditions from a single image.

**Cross-View Alignment.** Tackling data with related but different views has been an ongoing challenge, explored across various domains. For example, person re-identification methods [20, 34, 59, 67] aim to improve consistency for the same person across different cameras, cross-view image matching/retrieval [13, 52, 56] seeks to align images captured from different angles, and cross-view image translation [16, 29, 55] requires models to generate a novel view of an image while preserving its content. Image co-segmentation, such as SegSwap [51], which segments shared objects across various images, and video object tracking, such as XMem [3], which tracks objects across frames, seem to be the most closely related tasks to us. However, while these tasks share some similarities, we address fundamentally different challenges and employ distinct methodologies in our work.

### 3. Methodology

**Task Formulation.** The *Ego-Exo Object Correspondence* involves mapping objects between ego- and exo-centric video perspectives as in Fig. 1. Formally, given a query video  $V_{\text{query}}$  (e.g., an ego-centric or exo-centric video) and a target video  $V_{\text{target}}$  (e.g., an exo-centric or ego-centric video), along with object masks  $M_{\text{query}}$  indicating the object of interest in  $V_{\text{query}}$ , the objective is to predict the corresponding object masks  $M_{\text{target}}$  in  $V_{\text{target}}$ . The query and target videos are assumed to be temporally aligned, ensuring that corresponding frames represent the same time points. Additionally, each video pair may contain multiple objects of interest. Any semantic information e.g., the categories of the objects are not provided in the benchmark. Models are expected to leverage cross-view relationships to locate and segment the corresponding objects in the target perspective.

To structure and simplify usage, we rename the two sub-tasks as **Ego2Exo**, where the ego-centric video serves as the query and the exo-centric video as the target, and **Exo2Ego**, where the exo-centric video is the query and the ego-centric video is the target.

**PSALM Baseline.** As discussed in Sec. 2 and shown in Tab. 1, the UNINEXT [63], SEEM [69], PSALM [68] could be considered as the baselines. Among them, we select PSALM for its: 1) validated superior performance over UNINEXT and SEEM models on several various benchmarks; 2) demonstrated zero-shot learning (ZSL) transfer ability to our task. Particularly, PSALM combines Mask2Former [1], the potent generic segmentation model, with a powerful LLM leveraging the strengths of both. Briefly, PSALM first takes an image, an instruction prompt, a condition prompt (e.g., categories, text, or visual hint), and mask tokens as input to the LLM resulting in the condition embedding, mask embedding. It then predicts masks in a Mask2Former style based on the image and these LLM extracted embeddings. The model is trained by minimizing the loss,  $\mathcal{L}_{\text{mask}}$ , which is calculated by comparing the predicted masks to the ground truth.

#### 3.1. ObjectRelator Framework

Our proposed ObjectRelator operates at the frame level, focusing on studying object relations between ego-exo frames, leaving the exploration of temporal information as future work. The framework is illustrated in Fig. 2. Overall, we retain the core PSALM modules: Mask Token Extraction, Visual Encoder, MM (Multimodal) Projector, LLM, Pixel Decoder, Mask Generator, and also its loss function  $\mathcal{L}_{\text{mask}}$ , while introducing two novel components, **Multimodal Condition Fusion (MCFuse)** and **Cross-View Object Alignment (XObjAlign)**, highlighted in orange and light green colors.

For clarity, we use Ego2Exo as an example: each training step involves a synchronized ego image as the query and an exo image as the target. For each object in the paired data, we denote the ego image, ego object mask, exo image, and exo object mask as  $I^{\text{ego}}$ ,  $m^{\text{ego}}$ ,  $I^{\text{exo}}$ , and  $m^{\text{exo}}$  (ground truth), respectively. The following steps are:

**1) Preparing Inputs for LLM:** For the target exo image  $I^{\text{exo}}$ , we use the Visual Encoder, MLP Projector, and Pixel Decoder to extract features  $f_I^{\text{exo}}$  and  $f_I^{\text{exo}multi}$ , where  $f_I^{\text{exo}multi}$  indicates the feature has multiple layers. Unlike the ZSL PSALM model, which only uses the single ego object mask as a prompt for exo, we leverage both the visual object region and a language description as prompts. Thus, our instruction prompt  $P_{\text{ins}}$  is formulated as: “This is an image. Please segment by given regions and instruction.”,

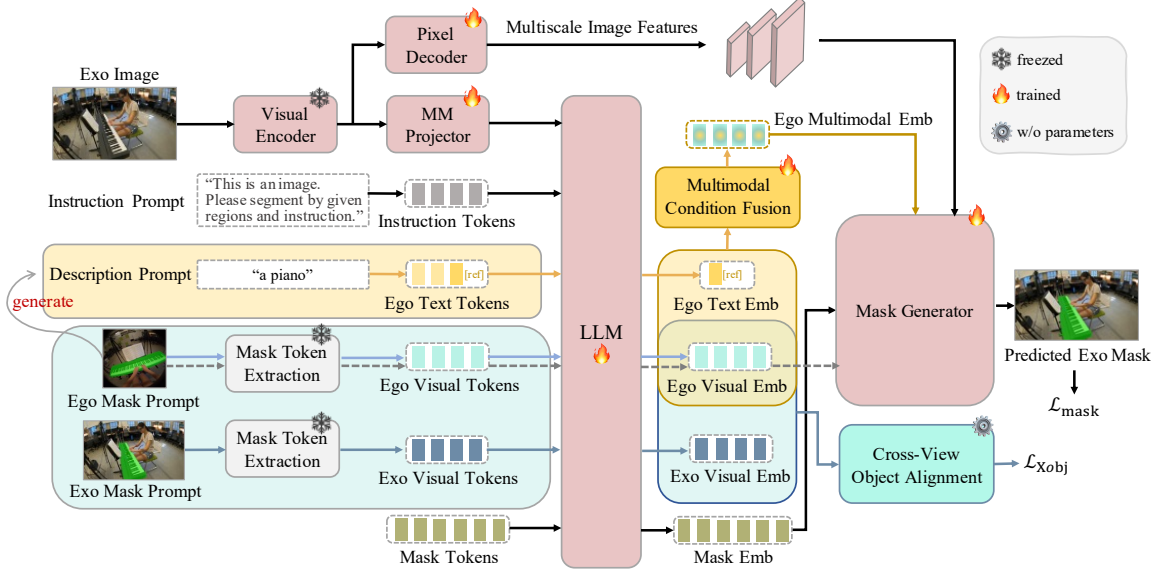


Figure 2. **Overview of ObjectRelator.** Ego2Exo is used as an example. The dashed lines mean the base PSALM relies solely on the ego mask prompt as the condition. The colorful lines represent our multimodal condition fusion and cross-view object alignment.

where the region hint is ego mask prompt  $P_V^{ego}$  and the instruction hint is the text instruction prompt  $P_T^{ego}$ . Specifically,  $P_V^{ego}$  is formed by combining the ego image  $I^{ego}$  and its object mask  $m^{ego}$ , while  $P_T^{ego}$  describes the masked object in  $I^{ego}$ , generated via the pre-trained multimodal model LLaVA [35]. Additionally, to enforce consistency between ego and exo objects, we use the ground truth  $m^{exo}$  to form the exo mask prompt  $P_V^{exo}$ . Note that although named a prompt,  $P_V^{exo}$  is not used for mask generation but only for the XObjAlign module. We then extract the instruction tokens  $T_{ins}$ , ego text condition token  $T_T^{ego}$ , ego visual condition token  $T_V^{ego}$ , exo visual token  $T_V^{exo}$ , and mask token  $T_M$ , following the same token extraction method e.g., the Mask Token Extraction module as the base PSALM.

**2) Forwarding the Network:** We process image features  $f_I^{exo}$ ,  $f_I^{exo_{multi}}$ , instruction tokens  $T_{ins}$ , ego text tokens  $T_T^{ego}$ , ego visual tokens  $T_V^{ego}$ , exo visual tokens  $T_V^{exo}$ , and mask tokens  $T_M$ . To feed these into the pretrained LLM, we create two inputs: one concatenating  $f_I^{exo}$ ,  $T_{ins}$ ,  $T_T^{ego}$ ,  $T_V^{ego}$ , and  $T_M$ , and the other with  $f_I^{exo}$ ,  $T_{ins}$ ,  $T_T^{ego}$ ,  $T_V^{exo}$ , and  $T_M$ . Feeding both inputs into the LLM yields ego text emb  $E_T^{ego}$ , ego visual emb  $E_V^{ego}$ , exo visual emb  $E_V^{exo}$ , and mask emb  $E_M$ . The embeddings  $E_V^{ego}$  and  $E_V^{exo}$ , representing the same object from different views, are passed through the XObjAlign module to compute the cross-object consistency loss  $\mathcal{L}_{Xobj}$ . Meanwhile,  $E_T^{ego}$  and  $E_V^{ego}$  are sent to the MCFuse module to generate the fused multimodal ego embedding  $E_{MM}^{ego}$ . Finally, the multiscale image feature  $f_I^{exo_{multi}}$ , the fused ego multimodal emb  $E_{MM}^{ego}$ , and the mask emb  $E_M$  are passed to the Mask Generator to predict the exo masks and compute the loss  $\mathcal{L}_{mask}$ .

**3) Training and Inference:** Our model has two training stages: a) **S1:** The MCFuse module is trained with the  $\mathcal{L}_{mask}$  loss to initialize it well for the second stage. b) **S2:** All modules (indicated by the fire icon) are trained jointly with the losses  $\mathcal{L}_{mask}$  and  $\mathcal{L}_{Xobj}$ . During inference, the XObjAlign module and also exo mask prompt  $P_V^{exo}$  are removed, and the remaining model is used for inference.

### 3.2. Key Module: Multimodal Condition Fusion

Our multimodal condition fusion (MCFuse) is mainly presented to break the limitation of the base model that only visual prompt is used, achieving the effective combination of the embedding from both text condition and visual mask condition. There are mainly two considerations for the design of MCFuse, 1) Given the extensive effectiveness of cross-attention in capturing intricate relationships across modalities, it serves as an ideal choice for fusing our multimodal conditions; 2) the model-generated texts can sometimes be unreliable, prioritizing visual information is prudent. This motivates our use of a residual design, with the visual input serving as the primary pathway. Additionally, to eliminate the need for manual tuning of the residual pathway’s weight, we introduce a learnable parameter,  $k_{lea}$ .

Formally, as shown in Fig. 3, given the ego text emb  $E_T^{ego} \in 1 \times D$  and ego visual emb  $E_V^{ego} \in N \times D$  as input, the cross-attention is applied to the broadcasted  $E_T^{ego}$  and  $E_V^{ego}$ , with  $E_T^{ego}$  serves as query,  $E_V^{ego}$  works as key and value. The fused result  $CA_{fuse}$  is given by:

$$CA_{fuse} = CrossAtt(E_T^{ego}W_Q, E_V^{ego}W_K, E_V^{ego}W_V) \quad (1)$$

where  $CrossAtt()$  means the cross attention,  $W_Q, W_K, W_V$



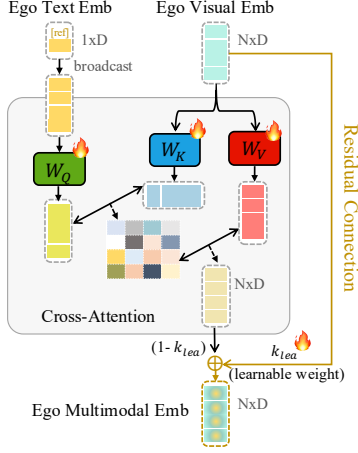


Figure 3. Architecture of our Multimodal Condition Fusion (MCFuse) module. All learnable sub-modules are denoted by fire icon.

denote the learnable parameters. After that, we combine the  $CA_{fuse}$  with the initial  $E_V^{ego}$  in a residual connection way with the learnable weight  $k_{lea}$  as,

$$E_{MM}^{ego} = k_{lea} \cdot E_V^{ego} + (1 - k_{lea}) \cdot CA_{fuse} \quad (2)$$

We highlight that though the base PSALM enables various condition prompts, they are never being used at the same time. While our MCFuse module proposes first to generate the text description for the masked object and then manage to fuse the multimodal conditions together.

### 3.3. Key Module: Cross-View Object Alignment

The Cross-View Object Alignment (XObjAlign) is mainly proposed to enhance the model’s consistent understanding of the same object but from totally different views i.e., ego-centric and exo-centric. The main insight behind this module is that a robust model should have a similar embedding for ego-masked object and also exo-masked object, and also considering the fact that the ego visual emb  $E_V^{ego}$  is working as the condition that directly affect the prediction of the Mask Generator. Thus, we propose to apply the consistency constraint exactly in the object visual embedding space.

As stated in the overview, to achieve such a consistency constrain, we propose to extract both the ego visual emb  $E_V^{ego}$  and exo visual emb  $E_V^{exo}$ , after that, the only thing left for the XObjAlign is to compare the similarities of these two embeddings and resulting in the cross-view object consistency loss  $\mathcal{L}_{Xobj}$  as,

$$\mathcal{L}_{Xobj} = Sim(E_V^{ego}, E_V^{exo}) \quad (3)$$

where the  $Sim()$  represents the similarity of the embedding features, and we use Euclidean distance to calculate it.

We highlight that though its simple design, the idea of aligning the cross-view object is worthy and our XObjAlign module enhances the model’s robustness on the view shift issue with no single additional parameter introduced.

## 4. Experiments

**Datasets.** We validate our method on the large-scale Ego-Exo4D [10], using its benchmark for ego-exo object correspondence tasks. The dataset contains 1.8 million annotated object masks at 1 fps across 1335 video takes, covering domains like Cooking, BikeRepair, Health, Music, Basketball, and Soccer. Each paired video features an average of 5.5 objects, tracked for an average of 173 frames. We use the standard Train/Val/Test splits but make the following adjustments: 1) To focus on cross-view segmentation, we retain only data where objects appear in both views; 2) We introduce a “Small” TrainSet (about one-third of the original “Full” TrainSet) for improved efficiency and data storage; 3) Testing is conducted on the Val set due to the lack of ground truth for the Test set. Our processed splits will be made available for future comparisons.

**Network Modules.** Following PSALM [68], we use Swin-B [37] as the Visual Encoder and Phi-1.5 1.3B [31] as the LLM. The MLP Projector, consisting of Conv2d, Batch-Norm2d, and FC layers, maps the visual latent space to the LLM space. The Pixel Decoder and Mask Generator are adapted from Mask2Former [1]. Mask Token Extraction is the same as PSALM, mainly applying average pooling of mask upon image features. MCFuse is described in Sec. 3.2, and XObjAlign requires no parameters.

**Implementation Details.** The pre-trained PSALM model serves as our initialization. In **S1** training, we use  $1/20$  of the training data to train MCFuse. In **S2** training, the full training set is used for optimizing all modules except the Swin-B vision encoder. Training details such as epochs, batch size, and learning rate are provided in the Appendix. All training runs on 4xA100 GPUs, while testing is conducted on a single A100, A6000, or L4 GPU. Training on Small TrainSet takes 5-6 hours, while training on the Full TrainSet takes around 20 hours.

### 4.1. Main Results on Ego-Exo4D

**Baselines and Competitors.** Directly aligned prior methods are quite limited, while still some efforts have been made. Specifically, 1) Ego-Exo4D [10] forms a spatial-based “XSegTx” method by adapting SegSwap [51], and two spatiotemporal-based “XView-XMem”, “XView-XMem + XSegTx” via adapting XMem [3] and combining it with “XSegTx”; 2) PSALM [68] tests its ZSL results; 3) In this paper, we also adapt and test the ZSL capabilities of SEEM [69], one additional universal segmentation method that decodes visual prompts by referring to the image. The adaption is mainly made by using the query view (e.g., ego in Ego2Exo) to generate the prompt for the target view (e.g., exo in Ego2Exo). Additionally, we retrain PSALM to form a more competitive baseline.

**Results on Ego-Exo4D.** The comparison results are summarized in Tab. 2, we indicate whether the method em-

Ego2Exo (Ego as Query)					Exo2Ego (Exo as Query)				
Method	ZSL	Type	TrainSet	IoU $\uparrow$	Method	ZSL	Type	TrainSet	IoU $\uparrow$
XSegTx* [10]	✓	S	-	0.3	XSegTx* [10]	✓	S	-	1.3
XSegTx* [10]	✗	S	Full	6.2	XSegTx* [10]	✗	S	Full	30.2
XView-Xmem* [10]	✓	ST	-	16.2	XView-Xmem* [10]	✓	ST	-	13.5
XView-Xmem* [10]	✗	ST	Full	17.7	XView-Xmem* [10]	✗	ST	Full	20.7
XView-Xmem + XSegTx* [10]	✗	ST	Full	36.9	XView-Xmem + XSegTx* [10]	✗	ST	Full	36.1
SEEM* [69]	✓	S	-	1.1	SEEM* [69]	✓	S	-	4.1
PSALM <sup>o</sup> [68]	✓	S	-	7.9	PSALM <sup>o</sup> [68]	✓	S	-	9.6
PSALM* [68]	✗	S	Small	39.7	PSALM* [68]	✗	S	Small	44.1
PSALM* [68]	✗	S	Full	41.3	PSALM* [68]	✗	S	Full	47.3
<b>ObjectRelator (Ours)</b>	✗	S	Small	<b>44.3</b>	<b>ObjectRelator (Ours)</b>	✗	S	Small	<b>49.2</b>
<b>ObjectRelator (Ours)</b>	✗	S	Full	<b>43.9</b>	<b>ObjectRelator (Ours)</b>	✗	S	Full	<b>50.9</b>

Table 2. Comparison results on Ego-Exo4D object correspondence benchmark. All the results are tested on the Val set. <sup>o</sup> means results from PSALM [68], • means results are reported by us.

employs ZSL learning, whether it is spatial-based (S) or spatio-temporal (ST) based, the TrainSet used, and most importantly its IoU metric. From the results, we first notice that our proposed ObjectRelator model significantly improves the base PSALM and achieves state-of-the-art performance on the ego-exo object correspondence task. Take models trained on Small TrainSet as an example, our ObjectRelator improves the PSALM from 39.7 to 44.3 on Ego2Exo and from 44.1 to 49.2 on Exo2Ego. These results well demonstrate the effectiveness of our proposed approach.

In addition to our SOTA results, several other key observations are as follows: 1) **ZSL Inference Performance:** Results show that nearly all the tested methods, including universal segmentation models like SEEM and PSALM, struggle to generalize smoothly to the ego-exo object correspondence task. While SEEM and PSALM excel on other out-of-domain tasks, such as open-vocabulary segmentation [6] and video object tracking [42], their performances are degraded here, highlighting the significant challenges posed by view shifts between ego and exo videos. This underscores that simply applying existing models, even those extensively pre-trained ones, is insufficient. Dedicated models specifically designed and trained for cross-view scenarios remain essential. XView-XMem shows the best ZSL performance, likely due to its video object tracking foundation. However, this advantage diminishes in the retrained XView-XMem. 2) **Baseline Retraining:** After retraining models on the benchmark, all baselines show reasonable performance, further emphasizing the importance of model adaptation for this task. In general, the superior performance of XView-Xmem and “XView-Xmem + XSegTx” over XSegTx suggests that temporal information aids cross-view alignment. However, this advantage can be offset by the model designs, as demonstrated by PSALM. The success of PSALM shows the effectiveness of interactive prompting, making it a strong baseline choice. 3) **Differences in Query Types:** Across models, performance is in general better on Exo2Ego than Ego2Exo, indicat-

ing that tasks with an ego-view query are more challenging. XSegTx exemplifies this disparity, achieving an IoU of 30.2 on Exo2Ego but only 6.2 on Ego2Exo. This aligns with intuitive expectations, as exo-view objects tend to be smaller and embedded within complex environments, increasing segmentation difficulty, while ego-view objects appear larger and more distinguishable from the background. 4) **Impact of Train Set Size:** Models trained on the Full TrainSet generally perform better, but we also observe that the Small TrainSet can effectively serve as a testbed for evaluating approaches, with results that approach and even occasionally exceed those of the Full TrainSet. This demonstrates the rationality of using Small TrainSet for efficient experimentation and evaluation, making it a practical alternative for benchmarking cross-view methods while reducing data requirements.

## 4.2. Ablation on Proposed Modules

**Effectiveness of the Proposed Modules.** To evaluate the contributions of every key component. Starting with the base PSALM, we incrementally added the MCFuse and XObjAlign to observe their individual impact. Results are reported in Tab. 3, in addition to the IoUs, the numbers of model parameters (No.Param.) are also provided.

Results show that: 1) Incorporating MCFuse into the base model significantly boosts performance, with clear improvements of 3.5 and 3.3 on Ego2Exo and Exo2Ego, respectively. This strongly supports our idea that introducing the language condition and effectively fusing it with the visual mask condition helps better identify the target object, particularly by reducing ambiguities. 2) Applying our XObjAlign module alone also brings significant improvements, boosting the base model by 4.1 and 4.2 on the two sub-tasks, surpassing even the benefits from MCFuse with its simpler design. These results highlight that narrowing the gap between ego and exo views is a key step toward building a more robust predictor. In our paper, we address or at least mitigate this gap by enforcing consistency between the

Method	MCFuse	XObjAlign	Ego2Exo $\uparrow$	Exo2Ego $\uparrow$	No.Param.
Base	$\times$	$\times$	39.7	44.1	1.5871B
+MCFuse	$\checkmark$	$\times$	43.2	47.4	+ 0.2632M
+XObjAlign	$\times$	$\checkmark$	43.8	48.3	+ 0
<b>ObjectRelator</b>	$\checkmark$	$\checkmark$	<b>44.3</b>	<b>49.2</b>	1.5873B

Table 3. Effectiveness of proposed modules. IoUs are reported. Methods trained on Small TrainSets. M/B means million/billion.

condition embeddings of ego and exo objects. 3) By integrating these two modules, our full ObjectRelator approach achieves the best results, indicating that the two modules are effectively compatible. However, we also observe that the combined effect is not simply additive. We interpret this as an overlap in the optimization directions of the two modules. For example, when the XObjAlign totally aligns the ego-exo views, the likelihood of the model misidentifying the objects across views is already low, which limits the capacity for the MCFuse to contribute further. This phenomenon demonstrates that both modules are working towards the model’s optimal solution from different perspectives. 4) Another point worth mentioning is that our method in total only introduces 0.2632M extra parameters, which is around 0.016% of the base PSALM while achieving 11.6% improvement on average.

**Further Ablations on Module Options.** To thoroughly assess the optimality of our design, we conduct additional ablation experiments applying various options to our modules. These include testing: whether cross attention (CA) is the best method for fusing conditions; the impact of adopting a learnable residual connection; the usage of the learnable weight; and the most suitable placement for applying XObjAlign. The results are presented in Tab. 4.

For the **fusion**-related experiments, we designed four variants: “Add”, “CA w/o Params”, “CA, S2”, “CA + LearnResidual, S2”. The “Add” method simply adds the ego text and visual conditions as an easy test of our generated text descriptions and also the idea of multi-condition fusion. The “CA w/o Params” variant applies cross-attention without parameters, formulated as  $(E_T^{ego} \cdot E_V^{egoT}) \cdot E_V^{ego}$ , which helps evaluate model sensitivity to added parameters. “CA, S2” represents standard cross-attention fusion, as shown in Eq. 3.2. “CA + LearnResidual, S2” uses our MCFuse module. The “S2” denotes that the entire network is trained only once (i.e., our second training stage). Results show: 1) Even simple methods like “Add” and “CA w/o Params” improve upon the base model, validating MCFuse’s core concept. 2) The notable drop with “CA, S2” suggests caution when introducing new parameters into other pre-trained modules, motivating our two-stage training strategy. This strategy is further validated by comparing “CA + LearnResidual, S2” with our MCFuse. 3) The improvement from “CA, S2” to “CA + LearnResidual, S2” supports protecting the more reliable visual prompt

Ablation Factor	Method	IoU $\uparrow$
	PSALM [68]	39.7
<b>Fusion</b>	Add	42.6
	CA w/o Params	42.1
	CA, S2	22.0
	CA+LearnResidual, S2	41.3
	CA+LearnResidual, S1-2 (Ours)	<b>43.2</b>
<b>Residual Weight</b>	$k = 0.2$	42.1
	$k = 0.5$	41.7
	$k = 0.8$	43.1
	$k_{lea}$ (Ours)	<b>43.2</b>
<b>Placement of XObjAlign</b>	After MCFuse	43.6
	Before MCFuse (Ours)	<b>44.3</b>

Table 4. Ablation study of proposed modules. Models are trained on Ego2Exo Small TrainSet.

condition. For the **residual weight** experiments, we compare our learnable approach with fixed weights  $k$  (0.2, 0.5, 0.8). Results indicate that learnable weight  $k_{lea}$  reduces manual tuning while effectively adapting to appropriate values. Regarding the **placement of XObjAlign**, we compare put XObjAlign “After MCFuse” with “Before MCFuse”. Results show the latter is more effective, likely because applying the alignment loss  $\mathcal{L}_{XObj}$  upon MCFuse may skew optimization toward better fusion objectives.

### 4.3. More Analysis

**Joint Training of Ego2Exo and Exo2Ego.** All previously reported results are obtained by training the Ego2Exo and Exo2Ego models separately, using their respective training sets. Thus, in this experiment, we investigate whether the training process can be merged by training a single model on both the Ego2Exo and Exo2Ego datasets simultaneously. The comparative results, shown in Tab. 5, confirm that the answer is yes. Our joint-trained models don’t degrade the performance of the separately trained models in most cases and even outperform the specific models. This suggests that the bidirectional correspondence learned during co-training helps the model understand the relationship between ego and exo perspectives more comprehensively.

Method	TrainSet	Training	Ego2Exo Testing	Exo2Ego Testing
<b>ObjectRelator</b>	Small	Ego2Exo	44.3	-
		Exo2Ego	-	49.2
		<b>Joint Training</b>	<b>44.7</b>	<b>50.6</b>
	Full	Ego2Exo	43.9	-
		Exo2Ego	-	<b>50.9</b>
		<b>Joint Training</b>	<b>46.7</b>	50.8

Table 5. Results of Joint Training on Small TrainSets.

### Single-Condition Evaluation of Multi-Condition Model.

Our proposed ObjectRelator is trained and tested with both visual mask and text description conditions. However, since text descriptions might not always be available, we are curious about what would happen if we test our multi-condition trained model using only the visual mask condition. To this

end, we evaluate the performance of removing the MCFuse module from our trained model, studying both the specific Ego2Exo and Exo2Ego models, as well as the joint-trained model. Results are summarized in Tab. 6.

The testing results show that while the performance with only the visual condition is inferior to using both visual and text conditions, the drop in performance is quite slight, and we still outperform the base PSALM model. This outcome exceeds our expectations, considering the inconsistency between training and testing conditions. Our interpretation is that, although we are exploring multimodal fusion rather than multimodal alignment, the model still manages to learn a joint space between the two different modality conditions. This enables the model to associate object categories with masks, allowing it to still perform well during testing, even when in the absence of text information.

Method	Training	Testing Conditions	Ego2Exo Testing	Exo2Ego Testing
PSALM [68]	Specific	Only Visual	39.7	44.1
		Visual + Text	<b>44.3</b>	<b>49.2</b>
ObjectRelator	Specific	Only Visual	43.3	48.9
		Visual + Text	<b>44.7</b>	<b>50.6</b>
	Joint	Only Visual	44.0	50.2

Table 6. Results of single condition testing. The studied Specific and Joint models are trained on Small TrainSets.

#### 4.4. Qualitative Results

To provide a more intuitive understanding of our method, we visualize the prediction results. Specifically, Fig. 4 presents several examples of ObjectRelator applied to both Ego2Exo and Exo2Ego tasks. The results indicate that our proposed methods perform effectively across diverse scenarios e.g., Basketball, Music, Cooking, and Bike Repair. Our method successfully segments objects in the target view despite significant size changes, shape variations, and cases where the query object is partially occluded. More visualization results can be found in the Appendix.

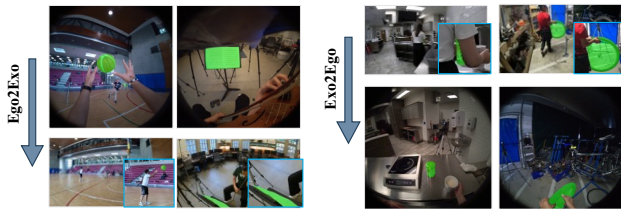


Figure 4. ObjectRelator Visualization for Ego2Exo and Exo2Ego.

To further demonstrate how our proposed modules improve upon the base PSALM, Fig. 5 compares the results between ObjectRelator and the retrained PSALM model, with ground truth provided as a reference due to the challenging nature of the examples. In Fig. 5(a), PSALM shows that PSALM will segment the wrong object with a similar shape to the query, as seen in the basketball and mu-

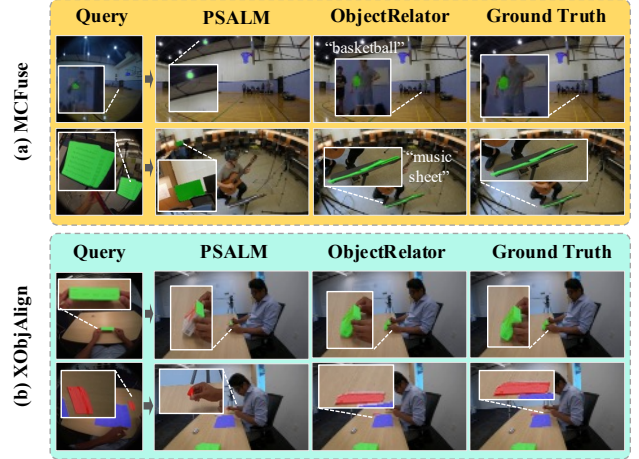


Figure 5. ObjectRelator vs. PSALM Visualization Results.

sic sheet examples. This indicates that relying solely on a visual mask fails to capture necessary semantic information. By contrast, our ObjectRelator, which leverages text descriptions to enhance the original visual mask condition, successfully corrects these errors in both examples, underscoring the effectiveness of our MCFuse module. Fig. 5 (b) presents examples where PSALM either segments only part of the target object (first example) or segments an incorrect object (second example). In both cases, the partially or incorrectly segmented object closely resembles the query object, suggesting that PSALM performs reasonably well but falls short in meeting the specific requirements of the ego-exo object correspondence task, where the same object may appear very different across views. The success of our method demonstrates the effectiveness of our proposed XObjAlign, which enforces consistency between ego and exo views as a solution.

#### 5. Conclusion

In this paper, we explored the Ego-Exo Object Correspondence task, a newly proposed and underdeveloped vision challenge. We introduced the ObjectRelator method, which incorporates two novel modules: Multimodal Condition Fusion (MCFuse) and SSL-based Cross-View Object Alignment (XObjAlign). MCFuse facilitates multi-condition fusion between language and visual modalities, while XObjAlign enforces consistency in object representation across different views through a self-supervised alignment strategy. Extensive experimental results demonstrate the effectiveness of our approach, showing significant improvements over the baseline and achieving state-of-the-art performance with minimal additional learnable parameters. As an early exploration of this task, we hope our work sparks further interest in this direction and paves the way for future research in comprehensive cross-view video applications.



## References

- [1] Bowen Cheng, Ishan Misra, Alexander G Schwing, Alexander Kirillov, and Rohit Girdhar. Masked-attention mask transformer for universal image segmentation. In *Proceedings of the IEEE/CVF conference on computer vision and pattern recognition*, pages 1290–1299, 2022. 1, 2, 3, 5
- [2] Feng Cheng, Mi Luo, Huiyu Wang, Alex Dimakis, Lorenzo Torresani, Gedas Bertasius, and Kristen Grauman. 4diff: 3d-aware diffusion model for third-to-first viewpoint translation. In *European Conference on Computer Vision*, pages 409–427. Springer, 2025. 2
- [3] Ho Kei Cheng and Alexander G Schwing. Xmem: Long-term video object segmentation with an atkinson-shiffrin memory model. In *European Conference on Computer Vision*, pages 640–658. Springer, 2022. 3, 5
- [4] Dima Damen, Hazel Doughty, Giovanni Maria Farinella, Sanja Fidler, Antonino Furnari, Evangelos Kazakos, Davide Moltisanti, Jonathan Munro, Toby Perrett, Will Price, et al. Scaling egocentric vision: The epic-kitchens dataset. In *Proceedings of the European conference on computer vision (ECCV)*, pages 720–736, 2018. 1, 2
- [5] Fernando De la Torre, Jessica Hodgins, Adam Bargteil, Xavier Martin, Justin Macey, Alex Collado, and Pep Beltran. Guide to the carnegie mellon university multimodal activity (cmu-mmact) database. 2009. 2
- [6] Zheng Ding, Jieke Wang, and Zhuowen Tu. Open-vocabulary universal image segmentation with maskclip. *arXiv preprint arXiv:2208.08984*, 2022. 6
- [7] Alireza Fathi, Ali Farhadi, and James M Rehg. Understanding egocentric activities. In *2011 international conference on computer vision*, pages 407–414. IEEE, 2011. 2
- [8] Yuqian Fu, Li Zhang, Junke Wang, Yanwei Fu, and Yu-Gang Jiang. Depth guided adaptive meta-fusion network for few-shot video recognition. In *Proceedings of the 28th ACM International Conference on Multimedia*, pages 1142–1151, 2020. 2
- [9] Kristen Grauman, Andrew Westbury, Eugene Byrne, Zachary Chavis, Antonino Furnari, Rohit Girdhar, Jackson Hamburger, Hao Jiang, Miao Liu, Xingyu Liu, et al. Ego4d: Around the world in 3,000 hours of egocentric video. In *Proceedings of the IEEE/CVF Conference on Computer Vision and Pattern Recognition*, pages 18995–19012, 2022. 1, 2
- [10] Kristen Grauman, Andrew Westbury, Lorenzo Torresani, Kris Kitani, Jitendra Malik, Triantafyllos Afouras, Kumar Ashutosh, Vijay Baiyya, Siddhant Bansal, Bikram Boote, et al. Ego-exo4d: Understanding skilled human activity from first-and third-person perspectives. In *Proceedings of the IEEE/CVF Conference on Computer Vision and Pattern Recognition*, pages 19383–19400, 2024. 1, 2, 5, 6
- [11] Abdul Mueed Hafiz and Ghulam Mohiuddin Bhat. A survey on instance segmentation: state of the art. *International journal of multimedia information retrieval*, 9(3):171–189, 2020. 2
- [12] Kaiming He, Georgia Gkioxari, Piotr Dollár, and Ross Girshick. Mask r-cnn. In *Proceedings of the IEEE international conference on computer vision*, pages 2961–2969, 2017. 1, 2, 3
- [13] Sixing Hu, Mengdan Feng, Rang MH Nguyen, and Gim Hee Lee. Cvm-net: Cross-view matching network for image-based ground-to-aerial geo-localization. In *Proceedings of the IEEE Conference on Computer Vision and Pattern Recognition*, pages 7258–7267, 2018. 3
- [14] Yifei Huang, Guo Chen, Jilan Xu, Mingfang Zhang, Lijin Yang, Baoqi Pei, Hongjie Zhang, Lu Dong, Yali Wang, Limin Wang, and Yu Qiao. Egoexolearn: A dataset for bridging asynchronous ego- and exo-centric view of procedural activities in real world. In *Proceedings of the IEEE/CVF Conference on Computer Vision and Pattern Recognition (CVPR)*, pages 22072–22086, 2024. 2
- [15] Vladimir Iashin and Esa Rahtu. Multi-modal dense video captioning. In *Proceedings of the IEEE/CVF conference on computer vision and pattern recognition workshops*, pages 958–959, 2020. 1, 2
- [16] Phillip Isola, Jun-Yan Zhu, Tinghui Zhou, and Alexei A Efros. Image-to-image translation with conditional adversarial networks. In *Proceedings of the IEEE conference on computer vision and pattern recognition*, pages 1125–1134, 2017. 3
- [17] Lixia Ji, Yunlong Du, Yiping Dang, Wenzhao Gao, and Han Zhang. A survey of methods for addressing the challenges of referring image segmentation. *Neurocomputing*, 583:127599, 2024. 2
- [18] Baoxiong Jia, Yixin Chen, Siyuan Huang, Yixin Zhu, and Song-chun Zhu. Lemma: A multi-view dataset for learning multi-agent multi-task activities. In *European Conference on Computer Vision*, pages 767–786. Springer, 2020. 2
- [19] Baoxiong Jia, Ting Lei, Song-Chun Zhu, and Siyuan Huang. Egotaskqa: Understanding human tasks in egocentric videos. *Advances in Neural Information Processing Systems*, 35: 3343–3360, 2022. 2
- [20] Xibin Jia, Xing Wang, and Qing Mi. An unsupervised person re-identification approach based on cross-view distribution alignment. *IET Image Processing*, 15(11):2693–2704, 2021. 3
- [21] Andrej Karpathy, George Toderici, Sanketh Shetty, Thomas Leung, Rahul Sukthankar, and Li Fei-Fei. Large-scale video classification with convolutional neural networks. In *Proceedings of the IEEE conference on Computer Vision and Pattern Recognition*, pages 1725–1732, 2014. 1, 2
- [22] Alexander Kirillov, Ross Girshick, Kaiming He, and Piotr Dollár. Panoptic feature pyramid networks. In *Proceedings of the IEEE/CVF conference on computer vision and pattern recognition*, pages 6399–6408, 2019. 1, 2
- [23] Alexander Kirillov, Eric Mintun, Nikhila Ravi, Hanzi Mao, Chloe Rolland, Laura Gustafson, Tete Xiao, Spencer Whitehead, Alexander C Berg, Wan-Yen Lo, et al. Segment anything. In *Proceedings of the IEEE/CVF International Conference on Computer Vision*, pages 4015–4026, 2023. 1, 2, 3
- [24] Kris M Kitani, Takahiro Okabe, Yoichi Sato, and Akihiro Sugimoto. Fast unsupervised ego-action learning for first-person sports videos. In *CVPR 2011*, pages 3241–3248. IEEE, 2011. 1, 2
- [25] Ranjay Krishna, Kenji Hata, Frederic Ren, Li Fei-Fei, and Juan Carlos Niebles. Dense-captioning events in videos. In

- Proceedings of the IEEE international conference on computer vision*, pages 706–715, 2017. 1, 2
- [26] Taein Kwon, Bugra Tekin, Jan Stühmer, Federica Bogo, and Marc Pollefeys. H2o: Two hands manipulating objects for first person interaction recognition. In *Proceedings of the IEEE/CVF International Conference on Computer Vision*, pages 10138–10148, 2021. 2
- [27] Xin Lai, Zhuotao Tian, Yukang Chen, Yanwei Li, Yuhui Yuan, Shu Liu, and Jiaya Jia. Lisa: Reasoning segmentation via large language model. In *Proceedings of the IEEE/CVF Conference on Computer Vision and Pattern Recognition*, pages 9579–9589, 2024. 1, 2, 3
- [28] Fahad Lateef and Yassine Ruichek. Survey on semantic segmentation using deep learning techniques. *Neurocomputing*, 338:321–348, 2019. 2
- [29] Weijia Li, Jun He, Junyan Ye, Huaping Zhong, Zhi-meng Zheng, Zilong Huang, Dahua Lin, and Conghui He. Crossviewdiff: A cross-view diffusion model for satellite-to-street view synthesis. *arXiv preprint arXiv:2408.14765*, 2024. 3
- [30] Xiangtai Li, Haobo Yuan, Wei Li, Henghui Ding, Size Wu, Wenwei Zhang, Yining Li, Kai Chen, and Chen Change Loy. Omg-seg: Is one model good enough for all segmentation? In *Proceedings of the IEEE/CVF Conference on Computer Vision and Pattern Recognition*, pages 27948–27959, 2024. 2, 3
- [31] Yuanzhi Li, Sébastien Bubeck, Ronen Eldan, AD Giorno, Suriya Gunasekar, and Yin Tat Lee. Textbooks are all you need ii: phi-1.5 technical report (2023). URL <https://arxiv.org/abs/2309.05463>. 5
- [32] Yin Li, Zhefan Ye, and James M Rehg. Delving into egocentric actions. In *Proceedings of the IEEE conference on computer vision and pattern recognition*, pages 287–295, 2015. 2
- [33] Kevin Qinghong Lin, Jinpeng Wang, Mattia Soldan, Michael Wray, Rui Yan, Eric Z Xu, Difei Gao, Rong-Cheng Tu, Wenzhe Zhao, Weijie Kong, et al. Egocentric video-language pretraining. *Advances in Neural Information Processing Systems*, 35:7575–7586, 2022. 1, 2
- [34] Shan Lin, Haoliang Li, Chang-Tsun Li, and Alex Chichung Kot. Multi-task mid-level feature alignment network for unsupervised cross-dataset person re-identification. *arXiv preprint arXiv:1807.01440*, 2018. 3
- [35] Haotian Liu, Chunyuan Li, Qingyang Wu, and Yong Jae Lee. Visual instruction tuning, 2023. 2, 4, 1
- [36] Jia-Wei Liu, Weijia Mao, Zhongcong Xu, Jussi Keppo, and Mike Zheng Shou. Exocentric-to-egocentric video generation. In *The Thirty-eighth Annual Conference on Neural Information Processing Systems*. 2
- [37] Ze Liu, Yutong Lin, Yue Cao, Han Hu, Yixuan Wei, Zheng Zhang, Stephen Lin, and Baining Guo. Swin transformer: Hierarchical vision transformer using shifted windows. In *Proceedings of the IEEE/CVF International Conference on Computer Vision (ICCV)*, 2021. 5
- [38] Hongchen Luo, Kai Zhu, Wei Zhai, and Yang Cao. Intention-driven ego-to-exo video generation. *arXiv preprint arXiv:2403.09194*, 2024. 2
- [39] Mi Luo, Zihui Xue, Alex Dimakis, and Kristen Grauman. Put myself in your shoes: Lifting the egocentric perspective from exocentric videos. In *European Conference on Computer Vision*, pages 407–425. Springer, 2025. 1, 2
- [40] Shervin Minaee, Yuri Boykov, Fatih Porikli, Antonio Plaza, Nasser Kehtarnavaz, and Demetri Terzopoulos. Image segmentation using deep learning: A survey. *IEEE transactions on pattern analysis and machine intelligence*, 44(7):3523–3542, 2021. 2
- [41] Hao Ouyang, Qiuyu Wang, Yuxi Xiao, Qingyan Bai, Juntao Zhang, Kecheng Zheng, Xiaowei Zhou, Qifeng Chen, and Yujun Shen. Codef: Content deformation fields for temporally consistent video processing. In *Proceedings of the IEEE/CVF Conference on Computer Vision and Pattern Recognition*, pages 8089–8099, 2024. 1, 2
- [42] Jordi Pont-Tuset, Federico Perazzi, Sergi Caelles, Pablo Arbeláez, Alex Sorkine-Hornung, and Luc Van Gool. The 2017 davis challenge on video object segmentation. *arXiv preprint arXiv:1704.00675*, 2017. 6
- [43] Shraman Pramanick, Yale Song, Sayan Nag, Kevin Qinghong Lin, Hardik Shah, Mike Zheng Shou, Rama Chellappa, and Pengchuan Zhang. Egovlpv2: Egocentric video-language pre-training with fusion in the backbone. In *Proceedings of the IEEE/CVF International Conference on Computer Vision*, pages 5285–5297, 2023. 2
- [44] Nishant Rai, Haofeng Chen, Jingwei Ji, Rishi Desai, Kazuki Kozuka, Shun Ishizaka, Ehsan Adeli, and Juan Carlos Niebles. Home action genome: Cooperative compositional action understanding. In *Proceedings of the IEEE/CVF Conference on Computer Vision and Pattern Recognition*, pages 11184–11193, 2021. 2
- [45] Hiba Ramadan, Chaymae Lachqar, and Hamid Tairi. A survey of recent interactive image segmentation methods. *Computational visual media*, 6(4):355–384, 2020. 2
- [46] Hanoona Rasheed, Muhammad Maaz, Sahal Shaji, Abdelrahman Shaker, Salman Khan, Hisham Cholakkal, Rao M Anwer, Eric Xing, Ming-Hsuan Yang, and Fahad S Khan. Glamm: Pixel grounding large multimodal model. In *Proceedings of the IEEE/CVF Conference on Computer Vision and Pattern Recognition*, pages 13009–13018, 2024. 1, 2, 3
- [47] Nikhila Ravi, Valentin Gabeur, Yuan-Ting Hu, Ronghang Hu, Chaitanya Ryali, Tengyu Ma, Haitham Khedr, Roman Rädle, Chloe Rolland, Laura Gustafson, Eric Mintun, Junting Pan, Kalyan Vasudev Alwala, Nicolas Carion, Chao-Yuan Wu, Ross Girshick, Piotr Dollár, and Christoph Feichtenhofer. Sam 2: Segment anything in images and videos. *arXiv preprint arXiv:2408.00714*, 2024. 2, 3
- [48] Krishna Regmi and Ali Borji. Cross-view image synthesis using geometry-guided conditional gans. *Computer Vision and Image Understanding*, 2019. 1
- [49] Zhongwei Ren, Zhicheng Huang, Yunchao Wei, Yao Zhao, Dongmei Fu, Jiashi Feng, and Xiaoje Jin. Pixellm: Pixel reasoning with large multimodal model. In *Proceedings of the IEEE/CVF Conference on Computer Vision and Pattern Recognition*, pages 26374–26383, 2024. 2, 3
- [50] Fadime Sener, Dibiyadip Chatterjee, Daniel Shelepov, Kun He, Dipika Singhania, Robert Wang, and Angela Yao. As-

- sembly101: A large-scale multi-view video dataset for understanding procedural activities. In *Proceedings of the IEEE/CVF Conference on Computer Vision and Pattern Recognition*, pages 21096–21106, 2022. 2
- [51] Xi Shen, Alexei A Efros, Armand Joulin, and Mathieu Aubry. Learning co-segmentation by segment swapping for retrieval and discovery. *arXiv*, 2021. 3, 5
- [52] Yujiao Shi and Hongdong Li. Beyond cross-view image retrieval: Highly accurate vehicle localization using satellite image. In *Proceedings of the IEEE/CVF Conference on Computer Vision and Pattern Recognition*, pages 17010–17020, 2022. 3
- [53] Gunnar A Sigurdsson, Abhinav Gupta, Cordelia Schmid, Ali Farhadi, and Karteek Alahari. Charades-ego: A large-scale dataset of paired third and first person videos. *arXiv preprint arXiv:1804.09626*, 2018. 2
- [54] Uriel Singer, Adam Polyak, Thomas Hayes, Xi Yin, Jie An, Songyang Zhang, Qiyan Hu, Harry Yang, Oron Ashual, Oran Gafni, et al. Make-a-video: Text-to-video generation without text-video data. *arXiv preprint arXiv:2209.14792*, 2022. 1, 2
- [55] Hao Tang, Dan Xu, Nicu Sebe, Yanzhi Wang, Jason J. Corso, and Yan Yan. Multi-channel attention selection gan with cascaded semantic guidance for cross-view image translation. In *CVPR*, 2019. 1, 2, 3
- [56] Yicong Tian, Chen Chen, and Mubarak Shah. Cross-view image matching for geo-localization in urban environments. In *Proceedings of the IEEE Conference on Computer Vision and Pattern Recognition*, pages 3608–3616, 2017. 3
- [57] Sergey Tulyakov, Ming-Yu Liu, Xiaodong Yang, and Jan Kautz. Mocogan: Decomposing motion and content for video generation. In *Proceedings of the IEEE conference on computer vision and pattern recognition*, pages 1526–1535, 2018. 1, 2
- [58] Xin Wang, Taein Kwon, Mahdi Rad, Bowen Pan, Ishani Chakraborty, Sean Andrist, Dan Bohus, Ashley Feniello, Bugra Tekin, Felipe Vieira Frujeri, et al. Holoassist: an egocentric human interaction dataset for interactive ai assistants in the real world. In *Proceedings of the IEEE/CVF International Conference on Computer Vision*, pages 20270–20281, 2023. 1, 2
- [59] Zheng Wang, Ruimin Hu, Chao Liang, Yi Yu, Junjun Jiang, Mang Ye, Jun Chen, and Qingming Leng. Zero-shot person re-identification via cross-view consistency. *IEEE Transactions on Multimedia*, 18(2):260–272, 2015. 3
- [60] Benita Wong, Joya Chen, You Wu, Stan Weixian Lei, Dongxing Mao, Difei Gao, and Mike Zheng Shou. Assistq: Affordance-centric question-driven task completion for egocentric assistant. In *European Conference on Computer Vision*, pages 485–501. Springer, 2022. 2
- [61] Jay Zhangjie Wu, Yixiao Ge, Xintao Wang, Stan Weixian Lei, Yuchao Gu, Yufei Shi, Wynne Hsu, Ying Shan, Xiao Hu Qie, and Mike Zheng Shou. Tune-a-video: One-shot tuning of image diffusion models for text-to-video generation. In *Proceedings of the IEEE/CVF International Conference on Computer Vision*, pages 7623–7633, 2023. 1, 2
- [62] Saining Xie, Chen Sun, Jonathan Huang, Zhuowen Tu, and Kevin Murphy. Rethinking spatiotemporal feature learning: Speed-accuracy trade-offs in video classification. In *Proceedings of the European conference on computer vision (ECCV)*, pages 305–321, 2018. 1, 2
- [63] Bin Yan, Yi Jiang, Jiannan Wu, Dong Wang, Ping Luo, Zehuan Yuan, and Huchuan Lu. Universal instance perception as object discovery and retrieval. In *Proceedings of the IEEE/CVF Conference on Computer Vision and Pattern Recognition*, pages 15325–15336, 2023. 2, 3
- [64] Antoine Yang, Arsha Nagrani, Paul Hongsuck Seo, Antoine Miech, Jordi Pont-Tuset, Ivan Laptev, Josef Sivic, and Cordelia Schmid. Vid2seq: Large-scale pretraining of a visual language model for dense video captioning. In *Proceedings of the IEEE/CVF Conference on Computer Vision and Pattern Recognition*, pages 10714–10726, 2023. 1, 2
- [65] Chuhan Zhang, Ankush Gupta, and Andrew Zisserman. Helping hands: An object-aware ego-centric video recognition model. In *Proceedings of the IEEE/CVF International Conference on Computer Vision*, pages 13901–13912, 2023. 1, 2
- [66] Ce Zhang, Changcheng Fu, Shijie Wang, Nakul Agarwal, Kwonjoon Lee, Chiho Choi, and Chen Sun. Object-centric video representation for long-term action anticipation. In *Proceedings of the IEEE/CVF Winter Conference on Applications of Computer Vision*, pages 6751–6761, 2024. 2
- [67] Guoqing Zhang, Zhun Wang, Jiangmei Zhang, Zhiyuan Luo, and Zhihao Zhao. Multi-scale image-and feature-level alignment for cross-resolution person re-identification. *Remote Sensing*, 16(2):278, 2024. 3
- [68] Zheng Zhang, Yeyao Ma, Enming Zhang, and Xiang Bai. Psalm: Pixelwise segmentation with large multi-modal model. In *European Conference on Computer Vision*, pages 74–91. Springer, 2024. 1, 2, 3, 5, 6, 7, 8
- [69] Xueyan Zou, Jianwei Yang, Hao Zhang, Feng Li, Linjie Li, Jianfeng Wang, Lijuan Wang, Jianfeng Gao, and Yong Jae Lee. Segment everything everywhere all at once. *Advances in Neural Information Processing Systems*, 36, 2024. 1, 2, 3, 5, 6



# ObjectRelator: Enabling Cross-View Object Relation Understanding in Ego-Centric and Exo-Centric Videos

## Supplementary Material

We first present the implementation details in Sec.6, followed by additional results in Sec.7, and conclude with a discussion of limitations and future work in Sec. 8.

### 6. Implementation Details

#### 6.1. Data Processing

**Frame Extraction.** We follow the same frame extraction process as the baselines, i.e., XSegTx, XView-Xmem, as provided by Ego-Exo4D [10]. Specifically, for both ego and exo views, we sample one frame every 30 frames in chronological order to ensure time synchronization. Meanwhile, since the resolution of ego and exo is different, we adopt different scaling ratios. For ego video, we scale its resolution from (1408, 1408) to (704, 704). While the exo video is scaled from (2160, 3840) to (540, 960).

**Train/Val/Test Sets.** As described in Sec. 4, we follow the same dataset splits as Ego-Exo4D [10], retaining only the ego-exo pairs where the object is visible in both views (in some cases, an object may be visible in one view but fully occluded in the other). To construct the **SmallTrain** set, we sample a subset of the **FullTrain** set at a fixed frequency of 1/3. In the end, for both Ego2Exo and Exo2Ego tasks, we have the **FullTrain**, **SmallTrain**, and **Val** sets. We further report the number of frame images (No. Img) and the average number of objects per frame (Avg. Obj) for each set in Tab. 7. All splits used in this work will be released to the community to facilitate reproduction and comparison.

	Ego2Exo			Exo2Ego		
	FullTrain	SmallTrain	Val	FullTrain	SmallTrain	Val
No. Img	110118	36706	31205	123381	41127	36073
Avg. Obj	2.4	2.4	2.4	2.3	2.3	2.3

Table 7. Number of images and average object per image of sets.

#### 6.2. Description Generation

**Using LLaVA for Object Descriptions.** Due to the lack of semantic information in the initial benchmark, we propose to utilize the pretrained vision language model LLaVA [35] for generating the text description to support the subsequence MCFuse module. Concretely, we merge the mask of the object of interest with the correspondence image to create the input. This approach not only directs the model’s attention to the masked area but also preserves the full contextual information, such as the background, which aids the model in better understanding the object. As for the text prompt, we use “*Identify the single object covered by the green mask without describing it. Note that it is not a*

*hand. Format your answer as follows: The object covered by the green mask is*”. By providing this text prompt and the masked image to LLaVA, we generate the corresponding object descriptions.

**Comparison Among Different Options.** We compare our way of generating text descriptions with two other options. Visual examples are provided in Fig. 6. Specifically: 1) **Without Object Masking (Fig. 6(a)):** The entire image is used as input without adding an object mask, and the prompt is: “*Could you help describe the main object of the image?*”. Results show that when the image contains multiple objects, the model struggles to identify the correct one. Attempts to zoom in on the target object lead to reduced resolution, making the image difficult for the model to interpret. 2) **With Object Masking but different prompt (Fig. 6(b)):** The object is masked, and the model is prompted with “*Please describe the object covered by the green mask.*” While this approach focuses the model’s attention on the masked area, it often incorrectly predicts the object as a human hand, which is not considered an object of interest in this benchmark. 3) **Our Approach (Fig. 6(c)):** We use an object-masked image as input and a prompt that explicitly excludes the human hand. Results show significant improvement, as the generated descriptions align with the target object categories in most cases.

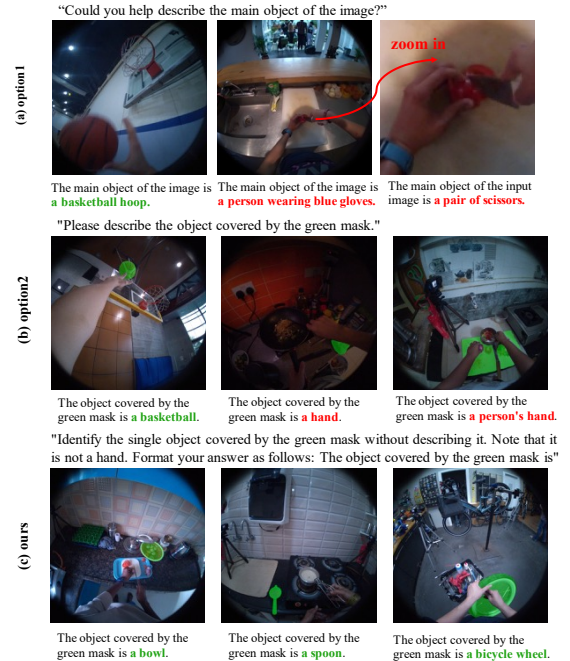


Figure 6. Comparisons among various options for text generation.



We acknowledge that the generated results are not always perfect; however, as demonstrated in Tab.2 and Tab.3, they have significantly contributed to improving performance. This validates our approach of leveraging textual information to enhance cross-view object understanding.

### 6.3. Training Details

Almost all models, including the base retrained PSALM, our ObjectRelator, and the ablation studies of ObjectRelator, share the same basic training setup: the pretrained PSALM model [68] is used as the initialization, AdamW is employed as the optimizer, the learning rate is set to  $6e-5$  with a cosine decay scheduler, the batch size is 12, and the image size is  $1024 \times 1024$ . By default, models without MCFuse are trained in a single stage (4 epochs) using all the data in the current training set. In contrast, models with MCFuse, such as our ObjectRelator, employ two training stages, **S1** and **S2**, with different epoch settings and data usage. The specific training configurations for our ObjectRelator are summarized in Tab. 8.

	Ego2Exo/Exo2Ego Training	Joint Training
<b>S1</b>	$1/20$ set, epoch = 4	$1/20$ set, epoch = 3
<b>S2</b>	all set, epoch = 4	all set, epoch = 3

Table 8. Training settings for ObjectRelator.

## 7. More Results

### 7.1. More Ablation Results

In Tab. 4, we present ablation studies exploring different configurations for our MCFuse module and the placement of MCFuse and XObjAlign. Additionally, we provide further ablation studies on the XObjAlign module, including various metrics for computing the consistency constraint and different weights for  $\mathcal{L}_{XObj}$ . Particularly, as in Tab. 9, we first compare the performance of using the Euclidean loss for XObjAlign with that of using cosine similarity, and then compare different weights for composing the sublosses  $\mathcal{L}_{mask}$  and  $\mathcal{L}_{XObj}$ . Note that only the XObjAlign module is applied. Results show that: 1) Compared to the cosine similarity, the Euclidean loss is better. However, both of them clearly outperform the base PSALM. 2) Among different choices, the default one  $\mathcal{L} = \mathcal{L}_{mask} + \mathcal{L}_{XObj}$  achieves the best result. The consistent improvement over the baseline observed across other weight ratios further demonstrates the robust positive impact of our XObjAlign module.

### 7.2. More Visualization Results

Due to space limitations, only a few examples are presented in Fig.4. To provide a more comprehensive view, we include additional visualization results in Fig.8 (Ego2Exo) and Fig. 9 (Exo2Ego). For each subtask, we showcase diverse examples spanning all six scenarios: Cooking, Bik-

Ablation Factor	Method	IoU $\uparrow$
-	Base PSALM [68]	39.7
Metrics for XObjAlign	Cosine	42.5
	<b>Euclidean (Ours)</b>	<b>43.8</b>
Loss Weights	$\mathcal{L} = \mathcal{L}_{mask} + 0.2 * \mathcal{L}_{XObj}$	41.2
	$\mathcal{L} = \mathcal{L}_{mask} + 0.5 * \mathcal{L}_{XObj}$	42.0
	$\mathcal{L} = \mathcal{L}_{mask} + \mathcal{L}_{XObj}$ ( <b>Ours</b> )	<b>43.8</b>
	$\mathcal{L} = \mathcal{L}_{mask} + 10 * \mathcal{L}_{XObj}$	40.3

Table 9. More ablation studies on XObjAlign and loss functions.

eRepair, Health, Music, Basketball, and Soccer. Results demonstrate that our proposed ObjectRelator effectively segments cross-view objects in most cases, producing results that closely align with ground truth annotations. This highlights the robustness of our method in handling diverse scenarios, various object categories, and challenging cases, such as occlusion and novel viewpoints.

## 8. More Discussions

**Failure Cases.** We also analyze the failure cases produced by our method, with typical examples summarized in Fig. 7. Results indicate that our method struggles in several scenarios: it fails to generate a complete mask when the object’s surface is discontinuous or blends closely with the background (first and third columns), incorrectly identifies the object when multiple similar objects are present in the scene (second and fourth columns), and occasionally misses some objects entirely (fourth column).

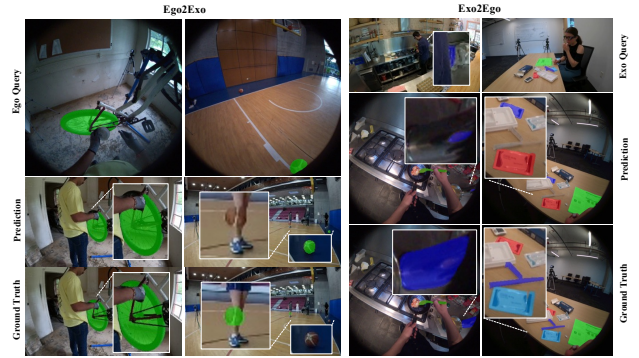


Figure 7. Visualization of failure cases. Ego2Exo/Exo2Ego models trained on SmallTrain sets are used.

**Limitations and Future Work.** In this paper, we propose ObjectRelator, a method designed to understand cross-view object relationships, particularly between ego-centric and exo-centric videos. The approach primarily consists of multimodal condition fusion and SSL-based cross-view object alignment, built on top of a frame-level segmentation model. While our method achieves SOTA results, as demonstrated in Fig. 7, there remains significant room for improvement. This underscores the substantial challenges and opportunities in addressing ego-exo object correspondence. Future work includes exploring diverse cross-view datasets and efficiently integrating temporal information.

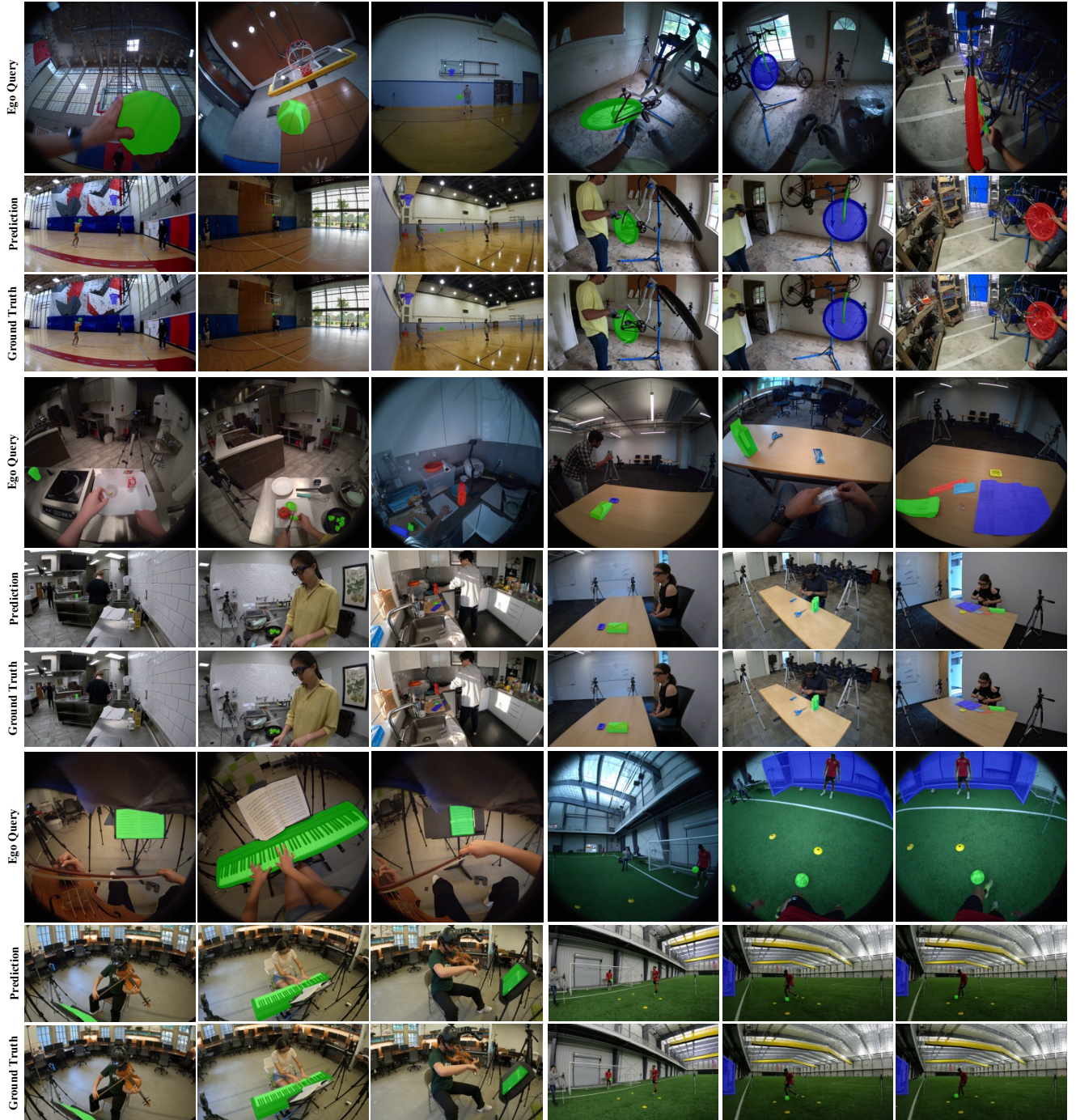


Figure 8. Ego2Exo visualization results (ego query, predictions, and ground truth). Ego2Exo model trained on SmallTrain set is used.





Figure 9. Exo2Ego visualization results (exo query, predictions, and ground truth). Exo2Ego model trained on SmallTrain set is used.